Available online at www.sciencedirect.com
SCIENCE DIRECT
Carbohydrate Polymers 60 (2005) 457–465
Carbohydrate Polymers
www.elsevier.com/locate/carbpol

Behavior of cellulose production of *Acetobacter xylinum* in ^{13}C-enriched cultivation media including movements on nematic ordered cellulose templates

Stephanie Hesse[a,b,*], Tetsuo Kondo[b,1]

[a]*Institute of Optics and Quantum Electronics, Friedrich Schiller University of Jena, Max-Wien-Platz 1, 07743 Jena, Germany*
[b]*Forestry and Forest Products Research Institute (FFPRI), Matusnosato 1, Tsukuba, Ibaraki 305-8687, Japan*

Received 2 February 2005; accepted 23 February 2005
Available online 29 April 2005

Abstract

Acetobacter xylinum NQ-5 (ATCC 53582) and AY-201 (ATCC 23769) cultivated in the Hestrin–Schramm medium containing D-glucose with a natural ^{13}C-abundance of 1.1% were investigated regarding their cell division rates and the bacterial movements. Comparative studies were carried out in the presence of D-glucose-U-$^{13}C_6$ with a uniform ^{13}C-labeling of 99% as the sole carbon source. The bacterial growth rates in numbers were found to increase in the ^{13}C-enriched media by about 13% for NQ-5 and 26% for AY-201, respectively. The movements of single cells caused by the inverse force of the secretion and deposition of cellulose nanofibers on nematic ordered cellulose (NOC) templates were investigated by real-time video analyzes using light microscopy. As a result, D-glucose-U-$^{13}C_6$ reduced the speed of motion for both strains, which was an opposite trend to the above growth rates in the cell division. The deposited cellulose fibers were proved to be in a cellulose crystalline form by CP/MAS ^{13}C NMR and NIR FT Raman spectroscopic measurements, although the biosynthesized and thereafter-deposited cellulose has a strong interaction with the surface of NOC.

Keywords: Bacterial cellulose; *Acetobacter xylinum*; ^{13}C-enriched cultivation; Nematic ordered cellulose (NOC); Template; Real-time video analysis; ^{13}C Nuclear magnetic resonance (NMR); NIR FT Raman

1. Introduction

The development of artificial materials for implantation based on bacterial cellulose has attracted much attention in the field of biomaterial science (Klemm, Schuhmann, Udhardt, & Marsch, 2001). *Acetobacter xylinum* (*A. xylinum*), a rod shaped, aerobic, gram negative bacterium, produces a cellulose nanofiber with 40–50 nm in width called 'bacterial cellulose ribbons' to be finally assembled as a white gelatinous material (pellicle) on the surface of the culture liquid in a static culture. Such native cellulose consists of sets of parallel chains of β-1,4-D-glucopyranose units interlinked by intermolecular hydrogen bonds. Fibrous structures with a certain ratio of crystalline and non-crystalline regions are formed, showing a large complexity and variability in their supramolecular arrangement. As formation as well as super- and supra-structure of bacterial cellulose fibers and pellicles can be controlled by the variation of the nutrient medium components and of the cultivation conditions (Klemm et al., 2001; Seifert, Hesse, Kabrelian, & Klemm, 2004), fundamental investigations of the biosynthesis and the microgravitative effects on the building of cellulose fibers are of special interest.

First, Brown, Willison, and Richardson (1976) reported the movement of *Acetobacter* in relation to cellulose biosynthesis in common Hestrin–Schramm (HS) cultivation media (Hestrin & Schramm, 1954). They found a cell movement rate of 2.0 μm per min at 25 °C due to an inverse force derived from the secretion of crystalline cellulose

* Corresponding author. Address: Centre of Excellence for Polysaccharide Research, Friedrich Schiller University of Jena, Humboldtstrasse 10, 07743 Jena, Germany. Tel.: +49 36 41 94 82 66; fax: +49 36 41 94 82 72.
E-mail address: stephanie.hesse@uni-jena.de (St. Hesse).
[1] Present address: Graduate School of Bioresources and Bioenvironmental Science, Kyushu University, 6-10-1 Hakozaki, Higashi-ku, Fukuoka 812-8581, Japan.

0144-8617/$ - see front matter © 2005 Elsevier Ltd. All rights reserved.
doi:10.1016/j.carbpol.2005.02.018

microfibrils by the bacterium. The secreted microfibrils are oriented in the same direction as the bacterium moves. The preparation of an artificially oriented film having molecular tracks termed nematic ordered cellulose (NOC) has been achieved (Kondo, Togawa, & Brown, 2001; Togawa & Kondo, 1999). The authors proposed that such oriented cellulose molecular tracks could be used as a template for the construction of 3-D regulated materials at a nano-scale. Namely, the direction of the secretion and the epitaxial deposition of cellulose nanofibers on NOC were controlled to follow the track direction, since the interactions between the produced cellulose fibers and specific sites of the oriented molecules on the unique surface of NOC were very strong. Moreover, Kondo et al. (2002) found that a cell movement rate of NQ-5 on NOC was ca. 4.5 μm per min at 24 °C.

The results on *A. xylinum* described above were achieved under normal conditions and using common D-glucose for the biosynthesis. To analyze the structure of bacterial cellulose in particular, isotopically exchanged samples are needed more often. Up to now, investigations on the labeling with carbon-13 are few (Arashida et al., 1993; Evans, Wang, Agblevor, Chum, & Baldwin, 1996; Gagnaire & Taravel, 1980; Kai et al., 1994, 1998). The finally obtained bacterial cellulose pellicles have been investigated regarding the transferring mechanisms of labeling from carbon to carbon. The ^{13}C-enriched samples are especially used for further structure analyzes by solid-state nuclear magnetic resonance (NMR) spectroscopy (Erata, Shikano, Yunoki, & Takai, 1997; Kono, Erata, & Takai, 2003; Kono et al, 2002). To investigate the supramolecular structure of cellulose, cross-polarization magic-angle-spinning (CP/MAS) ^{13}C NMR has been proven to be a powerful tool (Earl & VanderHart, 1980). It could be shown that naturally occurring cellulose I can be subdivided into cellulose Iα most abundant in cellulose from algae and bacteria and cellulose Iβ mostly found in cotton and higher plants (Atalla & Gast, 1980; Atalla & VanderHart, 1984; VanderHart & Atalla, 1984). The first assignment of the ^{13}C chemical shifts of the carbons C1 (96–108 ppm), C4 (81–93 ppm), and C6 (60–70 ppm) has been published by VanderHart and Atalla (1987). The overlapping resonances between 70 and 80 ppm were attributed to the carbon atoms C2, C3, and C5 without further identification. This assignment was confirmed later using selectively ^{13}C-labeled cellulose by Erata et al. (1997) and using solid-state INADEQUATE NMR by Lesage, Bardet, and Emsley (1999). Kono et al. (2002) found by ^{13}C-enriched material that two carbon signals appear for each carbon site in the structure, with the exception of C1 and C6 of cellulose Iα and C2 of cellulose Iβ with identical chemical shifts for the respective sites. Moreover, Kono et al. (2003) assigned the carbon signals to the carbon sites in the two different anhydroglucose rings of purified *Cladophora* (cellulose Iα) and *tunicate* (cellulose Iβ). Similarly, the line assignment has been carried out for bacterial cellulose (DSM 13368) using uniformly ^{13}C-enriched materials by Jaeger, Pauli, and Schmauder (2003).

Information on polymorphic changes in the structure of cellulose is essential for a better understanding of the process of biosynthesis. The supermolecular structure of each cellulose allomorph differs in their conformational arrangement of their side chains of the anhydroglucopyranose residues. In the range of the methylene bending vibrations, NIR FT Raman spectra indicate simultaneously presence of two stereochemically non-equivalent CH_2OH groups with the different rotation of the side chains about the C5–C6 atoms in cellulose I (Atalla, 1976; Atalla, Ranua, & Malcolm, 1984; Blackwell, Vasko, & Koenig, 1970). Thus, Raman spectroscopy is a suitable method for investigating the polymorphic characteristics.

In this study, the behavior of cellulose production of two strains of *A. xylinum*, NQ-5 (ATCC 53582) and AY-201 (ATCC 23769), was analyzed. Our goal was to show the influence of a modified carbon isotope distribution on biological systems. Therefore, HS media containing D-glucose-U-$^{13}C_6$ as the sole C-source were used for the biosynthesis of *A. xylinum* besides culture liquids containing common D-glucose. It should be ensured that the application of ^{13}C-enriched D-glucose does not have any influence on the microgravitative effects on the building of cellulose nanofibers. For this reason, primary experiments concerning the behavior of *A. xylinum* in ^{13}C-enriched culture liquids including growth rates and patterning of their movement on a specific template like NOC were of particular necessity. Besides, the supermolecular structure of the biosynthesized cellulose fibers was identified by NMR and NIR FT Raman spectroscopy. Further experiments on the morphology, molecular structure and crystallinity of *A. xylinum* pellicles grown on the ^{13}C isotope will be published elsewhere (Hesse, Togawa, & Kondo, in preparation).

2. Experimental section

2.1. Preparation of NOC templates

Nematic ordered cellulose (NOC) templates were prepared according to a previous method of Kondo et al. (2001) by stretching a water-swollen gel-like cellulose film that had been coagulated from dimethyl acetamide (DMAc)/LiCl solution. For this, lithium chloride dried at 105 °C was dissolved in anhydrous DMAc to give a concentration of 5% (w/w) solution (Togawa & Kondo, 1999). Dissolution of cellulose is basically followed by a previous swelling procedure using a solvent exchange technique (Chanzy, Peguy, Chaunis, & Monzie, 1980). The solution described above was poured into a surface-cleaned glass Petri dish with a flat bottom and placed in a closed box containing saturated water vapor at room temperature for a few days. In this manner, saturated water vapor slowly diffused into the solution and precipitated the cellulose. The precipitated

gel like films were washed with distilled running water for several days to remove the solvent. Thereafter, the water-swollen transparent gel-like films were cut into strips of about 30 mm in length and 5 mm in width, respectively. They were clamped in a manual-stretching device to be elongated uniaxially to a draw ratio of 2.0 at room temperature. The entire drawing process was completed with kept the specimen still wet. In the end, the never-dried NOC template was put into HS (Hestrin & Schramm, 1954) medium at pH 6.0, and the solvent was exchanged and finally maintained in a glass Petri dish until used for study.

2.2. Bacterial cultures

Two strains of *A. xylinum* of ATCC 53582 (NQ-5) with lengths of about 10 μm and ATCC 23769 (AY-201) with lengths of about 2 μm, respectively, were cultivated in tubes containing HS media in shaken cultures (30 °C, 200 rpm, 3 days, pH 6.0). Common D-glucose (^{13}C: 1.1%, natural abundance) and D-glucose-U-$^{13}C_6$ (^{13}C: 99%, uniformly labeled; Campro Scientific, Germany and Sigma-Aldrich Chemicals Co., USA) have been used as carbon sources. Steam sterilization of the culture liquid was carried out in an autoclave at 115 °C for 15 min. Two milliliters of the HS medium was inoculated with 40 μl of a 7-days-old liquid pre-culture of NQ-5 and AY-201, respectively.

For convenient cell's growth, 0.1 ml of the enzyme cellulase was added per 2 ml of cultivated HS medium. The growth rates of NQ-5 and AY-201 were compared regarding their cell division rates in both presence and absence of cellulase enzymes. After 3 days' incubation time, the medium had to be filtered using Nylon filters with a 40 μm pore in the mesh size in order to remove all possibly produced cellulose fibers. The remaining medium solution was centrifuged using a MX-300 by Tomy Digital Biology Co. Ltd., at 4 °C for 10 min with a rotation of 5000 rpm, in order to obtain the active bacteria. Thereafter, the enzyme cellulase was removed by alternate washing with distilled water and centrifugation as described above. After 3 times' washing, the bacteria were divided into tubes with 1 ml distilled water and kept at 4 °C until used for study. For light microscope observation, the distilled water was exchanged into the respective HS medium directly before the experiment.

During light microscope observations, *A. xylinum* biosynthesized cellulose nanofibers on the NOC template. The obtained cellulose samples by NQ-5 on NOC in common and in ^{13}C-enriched HS medium, respectively, were fixed in the manual-stretching device and air-dried at room temperature. Separately, cellulose fibers produced by NQ-5 in shaken cultures without cellulase were isolated by centrifugation, washed three times with distilled water, and air-dried at 60 °C.

2.3. Apparent cell numbers as relative values to be compared

The apparent number of cells per ml could be calculated by spectrophotometer (Hitachi U-3210) measurements of the optical density (OD) using the following equation

$$\frac{2.5\times10^{8}\ \text{cells/ml}}{0.3}=\frac{X}{\text{OD}}, \quad (1)$$

whereas X indicates the cells per ml, and OD is equivalent to the calculated absorption value of the spectrophotometer. The calculations are based on reference values of *colitis germ* at a wavelength of 600 nm (Morohoshi & Kimura, 2002).

2.4. Light microscopy (LM)

Real-time video analysis was made possible using images obtained by a Leica light microscope with L50×/0.55 objective lens, coupled with a ×1.25 optical lens, and with an Hamamatsu Photonics Co. (Shizuoka, Japan) cooled charge-coupled device camera, attached with a ×0.55 camera lens (HR 055-CMT) from Diagnostic Instruments (Sterling Heights, MI). Frames recorded every 20 s (three frames per min) were digitized, saved, and processed with IMAGE PRO PLUS 4.1 (Media Cybernetics). Samples observed were *A. xylinum* bacteria on substrates covered with HS medium, and kept just above the surface at 24 °C. The camera focus was set between the cells and the surface of the substrate, thus allowing the observation of both bacteria and biosynthesized cellulose nanofibers to be possible. Incident light in the system was minimized to prevent drying of the sample surface by the heat produced.

2.5. NMR spectroscopy

CP/MAS ^{13}C NMR spectra were recorded on a Bruker AMX 400 spectrometer operating at 100.58 MHz with a 4 mm MAS double resonance probe and ZrO_2 rotors. The sample spinning frequency was 6.5 kHz, the repetition time was 2 s and the cross polarization (CP) contact time was 1 ms. Per experiment, 20 k scans were accumulated, two-pulse phase modulation (TPPM: ±10°, 7 μs) has been applied for proton decoupling, and adamantane was used as an external reference having ^{13}C chemical shifts of 29.50±0.10 ppm (CH) and 38.56±0.10 ppm (CH_2) with respect to tetramethylsilane at 0.0 ppm (Earl & VanderHart, 1982).

2.6. NIR FT Raman spectroscopy

Raman spectra were recorded on a Bruker Equinox 55 (FRA 106/S with D 418-T) spectrometer with a liquid-nitrogen cooled Ge diode as a detector. A cw-Nd:YAG-laser operating at $\lambda_{\text{Nd:YAG}}=1064$ nm with a maximum power of 450 MW was used as light source for the excitation of

the Raman scattering. The spectra have been detected over the range of 3500–400 cm^{-1} using an operating spectral resolution of 4 cm^{-1} and averaged over 500 scans. The air-dried samples were placed across the sample holders.

3. Results and discussion

3.1. Growth rates in cell division of A. xylinum

To apparently determine the cell division rates, shaken cultures were analyzed by spectrophotometer measurements. Furthermore, the cultivated HS medium enriched by cellulase was compared with liquid cultures without enzyme. As described by Emert, Grum, Lang, Liu, and Brown (1974) and Whitaker (1971), cellulase refers to a group of enzymes which, acting synergistically, hydrolyzes cellulose. The enzymatic mechanism whereby certain microorganisms can quite rapidly and completely degrade cellulose has not yet been clearly understood. There are at least two steps involved (Reese, Siu, & Levinson, 1950): a pre-hydrolytic step wherein anhydroglucose chains are swollen or hydrated, and the subsequent hydrolytic cleavage of this susceptible polymers either randomly or endwise.

In our case, cellulase effected an almost complete decomposition of the biosynthesized cellulose fibers, usually resulting in more encouraging either cell division or production of the fibers in *A. xylinum*. After 3 days' incubation time, the cultivated HS medium was not clear anymore, but clouded by macroscopic particles due to very short cellulose 'fiber-dots' attached to the cells. The clouding process was observable for both NQ-5 and AY-201 in normal and in ^{13}C-enriched culture liquids. Thus, spectrophotometer measurements allowed a comparison between the two types of strains in *A. xylinum* relating to the medium used. In case of a cellulase-free system, cells with short cellulose fibers creating a kind of clews were observed.

There were significant differences between the cell division rates in common and ^{13}C-enriched HS media. According to Table 1, the growth rates of bacteria in liquid cultures with the enzyme were dependent on the carbon isotope distribution of the medium. For both NQ-5 and AY-201, it was shown that the cell division of bacteria growing up with addition of the enzyme depended on the available D-glucose for their metabolisms and occurred faster using ^{13}C-labeled D-glucose for the culture liquid. In the case of NQ-5, the number of cells per ml increased by about 13% using D-glucose-U-$^{13}C_6$ when compared with a case in the usual HS medium system, and for AY-201 this value was even higher (26%). A possible explanation could be that bacteria were forced to divide by reaching a certain body weight. Furthermore, there was an explicit difference observable by comparing the cell number per ml in the enzyme-added and enzyme-free HS media. Only about the half of the cells could be detected in the case of cellulase-free, but it is still difficult to prove whether this fact was due to the missing enzyme or not. The reduction of the cell number might be explained by the loss of active bacteria by the filtering procedure, so that the cells surrounded by their own fiber clew got lost using filters with a 40 μm pore in the mesh size. When the enzyme was omitted, the number of cells per ml decreased from $\Delta_{NQ\text{-}5}=(1.59\pm0.17)\times10^8$ to $(0.80\pm0.19)\times10^8$ for NQ-5. However, the reduction in the number of AY-201 cells, which also possibly got lost by filtering, was less than that in the cell number of NQ-5. This fact could be due to the significant smaller size of AY-201 cells that could pass through the filter.

Table 1
The averaged cell division rates of *A. xylinum* (Δ in cells/ml) in shaken tubes with 2 ml HS medium and 40 ml preparatory culture of NQ-5 and AY-201, respectively, after 3 days' incubation time

C-source of the HS medium	Cellulase (%) (w/w)	$\Delta_{NQ\text{-}5}$ (cells/ml)$\times10^{-8}$	$\Delta_{AY\text{-}201}$ (cells/ml)$\times10^{-8}$
D-glucose	–	0.80 ± 0.19	1.12 ± 0.21
	5	1.59 ± 0.17	1.63 ± 0.14
D-glucose-U-$^{13}C_6$	5	1.80 ± 0.17	2.06 ± 0.16

A measurement of each experiment was repeated at least five times; thus the standard deviations are given.

3.2. Bacterial movements on NOC

To calculate the moving rates of bacteria, light microscopy was used. Our template NOC having a specific molecular ordering as molecular tracks was made from cellulose as described previously (Kondo et al., 2001, 2002). When active bacteria of a strain of *A. xylinum* are transferred onto the oriented surface of NOC, they start to biosynthesize cellulose nanofibers parallel to the molecular track orientation of the surface (Togawa & Kondo, 1999). To observe the bacterial movements, an appropriate experimental arrangement was necessary, as shown in Fig. 1, in order to protect NOC as well as *A. xylinum* against drying due to the heat by incident light for the microscopic observation. Fifty microliter of the common and the ^{13}C-enriched culture liquid, respectively, has been given on top of the NOC, and 10 μl of the culture liquid including *A. xylinum* was added finally.

The typical movement of *A. xylinum* NQ-5 on NOC as well as their fiber production is in the following:

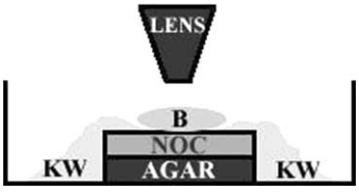

Fig. 1. Experimental arrangement for the light microscope observations. A thin paper (Kim wipes©: KW) soaked by a common and ^{13}C-enriched HS medium, respectively, were used to protect NOC as well as *A. xylinum* bacteria (B) in the respective medium against drying.

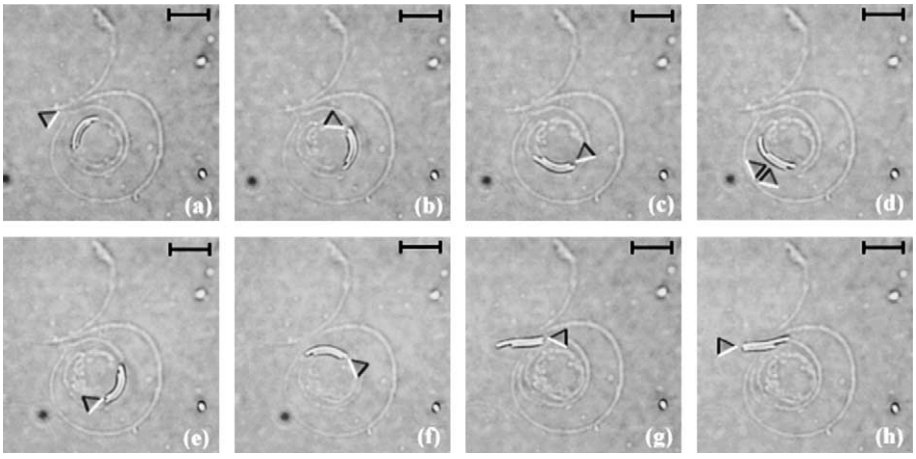

Fig. 2. Light microscope observations of the movement of a couple of *A. xylinum* NQ-5 within a real time of 4220 s. The individual frame was recorded every 20 s, whereas eight frames of 211 were selected. The interval between the displayed frames was not constant. The scale is showing the range of 10 μm.

Bacterial-synthesized cellulose nanofibers are first attached to monomolecular tracks of NOC, inducing a motion of the cells along the track direction. In midway of this movement, they sometime jumped off the tracks (not shown in this article). After jumping off the tracks, the bacteria start to change their orientation, and generate some kinds of spirals. In this way, bacterial movement is not necessarily straight-path. It was also found that *A. xylinum* are first going on NOC tracks, then describing spirals, and going forward and backward many times, as published previously (Kondo et al., 2002). The present study showed that this pattern of movements did not depend on difference between ^{12}C- and ^{13}C-enriched D-glucose used for the culture liquid. As a new result, it could be demonstrated that the bacteria were addicted to contact one another, once they were coupled on NOC.

Fig. 2(a) shows two NQ-5 bacteria in common HS medium that were touched to each other. The couple moved on spirals several times, which was proved by their own deposited cellulose nanofibers on NOC. Obviously, they had already jumped off the monomolecular tracks. The pictures (b) and (c) show them generating a spiral, and (d) is an example for moving forward and backward while the bacteria were touched to each other. This motion in (d) indicated a kind of rubbing with each other, whereas the cells did not leave their place. After a couple of seconds, the bacteria stopped rubbing, and simultaneously started to move reversely in the same direction of their primal rotation in (a)–(c). Now in Fig. 2(e)–(g), they again turned back on almost the same route of their deposited cellulose spiral pattern. In the end, picture (h) shows the combined change of a direction of the movement in both bacteria again.

The frames of Fig. 3 clarify the movement of a single cell as well as its ribbon production in particular. Such an observation allows an exact determination of the moving rate by analyzing the deposited fiber length within the respective observation time. As the individual frame was recorded every 20 s, the observation time can be calculated by multiplying the number of frames by 20 s. The calculations were done in a uniform manner for both strains of *A. xylinum*.

For NQ-5, it was observable that the motion of bacteria corresponded to their produced cellulose deposition on NOC. As listed in Table 1, D-glucose-U-$^{13}C_6$ activated the division of NQ-5 cells. In addition, the movement of a single bacterium was influenced by the ^{13}C-enrichment, as shown in Table 2. Light microscope observations of a single bacterium demonstrated that *A. xylinum* NQ-5 grown up and observed in common HS medium exhibited highest production and moving rates of 4.2 ± 0.4 μm/min on NOC, which agrees with a previous datum (Kondo et al., 2002). Furthermore, NQ-5 observed in common HS media on NOC following activated incubation in ^{13}C-enriched media showed an even higher production rate (3.1 ± 0.2 μm/min) than those treated with both incubation and observation in the same ^{13}C-enriched culture liquids

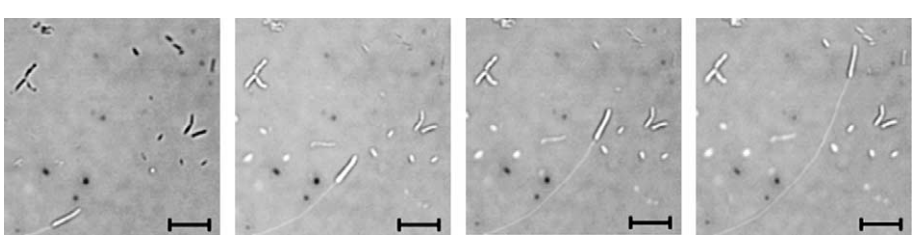

Fig. 3. Light microscope observations of the movement of a single AY-201 bacterium within a real time of 480 s. The individual frame was recorded every 20 s, whereas four frames of 24 were selected. The interval between the displayed frames was not constant. The scale is showing the range of 5 μm.

Table 2
The averaged speeds of motion of *A. xylinum* on NOC templates (v in (μm/min))

C-source of the HS medium for		v_{NQ-5} (μm/min)	v_{AY-201} (μm/min)
Cultivation of *A. xylinum*	Light microscope observations		
D-glucose	D-glucose	4.2±0.4	3.2±0.5
D-glucose-U-$^{13}C_6$		3.1±0.2	–
	D-glucose-U-$^{13}C_6$	2.1±0.5	2.2±0.3

A measurement of each experiment was repeated at least eight times; thus the standard deviations are given.

(2.1±0.5 μm/min). This means that the movement of a single cell was decelerated by D-glucose-U-$^{13}C_6$, and so the cellulose production of the bacterium also was.

AY-201 strain showed the same behavior as NQ-5 strain, cf. Table 2. The production rate of AY-201 observed in common HS media on NOC following activated incubation in ^{13}C-enriched media was considerably higher (3.2± 0.5 μm/min) than the rate of cells grown up and observed in the same ^{13}C-enriched media (2.2±0.3 μm/min). Thus, the movement of a single AY-201 bacterium was also decelerated by the ^{13}C-enrichment as found for NQ-5.

The previous paper (Kondo et al., 2002) suggested that the cell movement may be enforced by the directed polymerization and crystallization of cellulose ribbons. The rate was not always constant for each strain of *A. xylinum*. When they were moving on NOC covered by a common HS medium, AY-201 bacteria were in general slower than NQ-5. This could be partly due to the smaller size of their secreted cellulose nanofibers since bacterial motion is due to the inverse force derived from secretion of cellulose microfibrils by the cell.

Interestingly, both NQ-5 and AY-201 strains moved on NOC templates in the HS media with D-glucose-U-$^{13}C_6$ at almost the same velocity of ca. 2 μm/min. Because of the different masses of carbon isotopes (m_{13_C} = 13.00335 Dalton = 1.0836125 m_{12_C}), bacteria grown up in a ^{13}C-enriched HS medium as well as their produced cellulose ribbons are heavier than those in a common culture liquid without the ^{13}C-enrichment. Assuming that the rate of bacterial motion corresponds to the secretion rate of cellulose nanofibers by a cell, the additional weight due to the ^{13}C-enrichment could cause a slower motion of the bacteria.

3.3. Supermolecular structure of the deposited cellulose nanofibers on NOC

Previously (Kondo et al., 2002), it has been published that the deposited fiber on NOC was not a normally self-aggregated ribbon-like bacterial cellulose fiber anymore. The width of the NOC-altered fibers was 500–700 nm with splayed nanofibers having 7–8 nm apart. Usually, the width of cellulose ribbons is about 40–60 nm. Thus, it is of great importance to analyze the fiber structure of just biosynthesized and deposited cellulose nanofibers on the surface of NOC by spectroscopic methods such as NMR and NIR FT Raman, even though the amount of the deposited fibers on the very surface of NOC was quite small. All the obtained data were also to be compared with those for crystalline bacterial cellulose fibers or pellicles.

The CP/MAS ^{13}C NMR experiments were carried out to investigate the structural characteristics of cellulose nanofibers biosynthesized and deposited by NQ-5 on NOC in common and in ^{13}C-enriched HS media. The spectra were compared with ^{13}C NMR spectra of 14-days-old cellulose pellicles of static cultures produced by NQ-5 in common and in ^{13}C-enriched culture liquids, cf. Hesse et al. (in preparation).

For the never-dried bacterial cellulose pellicle from NQ-5 in Fig. 4(a), the ^{13}C-chemical shifts could be assigned to the carbons of the crystalline parts as follows: C1(β) [106.1 ppm]; $C1_{1,2}(\alpha)$ [105.5 ppm]; C1′(β) [104.4 ppm]; $C4_1(\alpha)$ [90.1 ppm]; $C4_2(\alpha)$ and C4(β) [89.3 ppm]; C4′(β) [88.5 ppm]; C3′(β) [75.9 ppm]; $C3_1(\alpha)$ [75.0 ppm]; $C3_2(\alpha)$ and C3(β) [74.5 ppm]; $C5_2(\alpha)$ and C5(β) [72.9 ppm]; $C2_1(\alpha)$, C2(β), C2′(β) and C5′(β) [72.0 ppm]; $C2_2(\alpha)$ and $C5_1(\alpha)$ [71.1 ppm]; $C6_{1,2}(\alpha)$, C6(β) and C6′(β) [65.6 ppm]. Non-crystalline cellulose parts were found around 83.9 ppm (C4 region) and 61.6 ppm (C6 region). It is noted that in the wet state sharpness and resolution of the multi-component lines of the ^{13}C NMR spectra were much better than in the dried state, however, the drying procedure did not alter the isotropic values as found by Hesse and Jaeger (2005). Using a line shape analysis, the cellulose I-type with a high content of the Iα-allomorph could be proved for the cellulose pellicle biosynthesized by NQ-5 in HS medium containing D-glucose-U-$^{13}C_6$, as shown in Fig. 4(b). As for common bacterial cellulose from NQ-5, the quantitative analysis of the C4 resonances for the crystalline (around 90 ppm) and non-crystalline (at about 84 ppm) regions indicated that

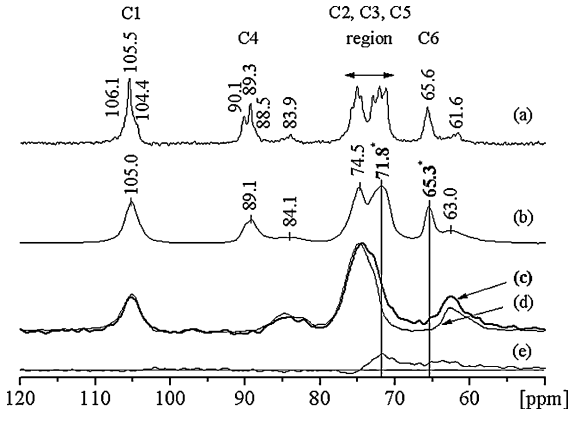

Fig. 4. CP/MAS ^{13}C NMR spectra of pellicles of (a) never-dried bacterial cellulose NQ-5 and (b) air-dried bacterial cellulose NQ-5 biosynthesized with D-glucose-U-$^{13}C_6$ (Hesse et al., in preparation), and CP/MAS ^{13}C NMR spectra of NOC with the deposited cellulose nanofibers produced by NQ-5 in (c) ^{13}C-enriched culture liquid and (d) common HS medium, showing their difference spectrum (e).

only about 1/4 of the ^{13}C-labeled bacterial cellulose was found in non-crystalline regions. The resolution of the lines is limited due to the strong homonuclear dipolar carbon–carbon couplings in the uniform ^{13}C-enriched sample. However, the line shape analysis allowed the assignment of the ^{13}C-chemical shifts to refer to the carbons in the crystalline regions of the never-dried bacterial cellulose mentioned above, and furthermore, there was no significant shift in their isotropic values. As NOC is a highly ordered but non-crystalline form of cellulose, the ^{13}C-chemical shifts could be assigned to the carbon sites as follows: C1-[108.5···102.5 ppm], C4- [88.6···80.0 ppm], C2, C3, C5-[79.5···67.6 ppm], and C6-regions [66.2···57.5 ppm]. The CP/MAS ^{13}C NMR spectra of cellulose nanofibers deposited on NOC in Fig. 4(c) and (d) were supposed to involve the spectrum of such ordered cellulose. In fact, using the common HS medium, no cellulose fibers could be detected by ^{13}C NMR, since the amount of produced cellulose nanofibers on NOC was just not enough, cf. Fig. 4(d). Using D-glucose-U-$^{13}C_6$ for the culture liquid, the ^{13}C NMR lines of the cellulose nanofibers deposited on NOC in Fig. 4(c) were widened, which might be due to the produced ^{13}C-labeled fibers. Some slight differences were observed in the C6 position, and a line broadening of the shift due to C2, C3, and C5 occurred, as shown in the difference spectrum in Fig. 4(e). Those additional resonances were comparable to the lines around 71.8 and 65.3 ppm of the ^{13}C-labeled bacterial cellulose pellicle in Fig. 4(b), indicating crystalline regions. Thus, the biosynthesized fibers on NOC appear to be of crystalline bacterial cellulose even though their self-aggregation was inhibited by the strong interaction between the biosynthesized microfibrils and the NOC surface causing much wider deposited fibers (hundreds of nanometer in width) along the molecular track direction of NOC.

Due to the very small amount of biosynthesized cellulose nanofibers deposited on NOC, it was not possible to investigate them by NIR FT Raman spectroscopy. Therefore, this technique was applied to analyze the 3-days-old cellulose fibers produced by NQ-5 in shaken cultures instead of the NOC surface. The spectrum clearly demonstrated the vibrational behavior depending on the polymorphic state of the cellulose. A cross in Fig. 5 denoted the typical assignments due to those phases of cellulose in the Raman spectrum. The assignment of these vibrational modes can be derived from the literature (Atalla, 1976; Blackwell et al., 1970; Wiley & Atalla, 1987).

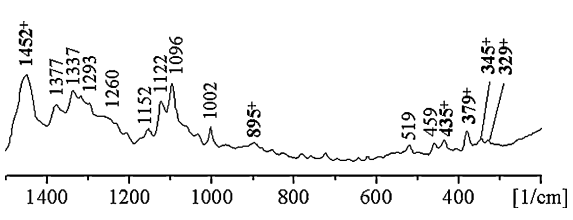

Fig. 5. NIR FT RAMAN spectrum of cellulose fibers produced by NQ-5 strain in the common HS medium after 3 days' incubation time in a shaken culture.

Here, we focused on the vibrational modes in the conformationally sensitive range below 1500 cm^{-1} only that are favorable for characterizing polymorphic changes. The denoted wave numbers of the Raman spectrum of the produced cellulose fibers in Fig. 5 clearly indicated the vibrational frequencies characterizing cellulose I crystalline phase. The predominantly internal coordinates of the frequency range of 1500–800 cm^{-1} are due to modes involving considerable couplings of methane bending, methylene rocking and wagging, and COH in-plane bending vibrations. Except for the internal modes of the CH_2OH groups, all motions were quite delocalized. The results of the present Raman spectrum were in good agreement with the published data of bacterial cellulose (Schenzel & Fischer, 2001) even though just medium–weak intensity bands could be detected below 1400 cm^{-1} compared with the band at 1452 cm^{-1}. Interestingly, the Raman peak at 895 cm^{-1} inversely correlated with the lateral size of the cellulose crystallites (Wiley & Atalla, 1987), was of very low intensity. ^{13}C NMR experiments of native celluloses suggested that the intensity of this band is proportional to the amount of disorder in cellulose (VanderHart & Atalla, 1984). Thus, the weak Raman peak at 895 cm^{-1} was another indication of the high order of crystalline state of the biosynthesized cellulose fibers. The vibrational spectrum of the bacterial cellulose in the range of skeletal deformations was characterized by typical Raman peaks: 435, 379, 345, and 329 cm^{-1}. Comprising, the typical Raman spectrum of a crystalline state of bacterial cellulose could be detected for the 3-days-old cellulose fibers. Referring to the nanofibers on the NOC template, we suppose that such typical Raman peaks should be also detected if the sample amounts were enough for investigations. In particular, as CP/MAS ^{13}C NMR suggested crystalline phases in the directly deposited fibers on NOC, the Raman results of cellulose fibers were a portent of the crystalline character of nanofibers.

4. Conclusion

The growth rate of the cell division in *A. xylinum* was dependent on the kind of strains in the bacterium and the type of D-glucose used for bacterial metabolisms when the cells grew up with added enzyme of cellulase. Both NQ-5 and AY-201 strains divided faster in a ^{13}C-enriched than in a common HS medium. Up to now, no explanation for this phenomenon is possible. A faster growth rate may be connected with the production of cellulose fibers in the bacterium that corresponds to a rate of the bacterial motion. In fact, the ^{13}C-enrichment played an important role in the movement of a single cell. The bacterial motion due to the inverse force derived from the secretion of cellulose ribbons by the cell was influenced by

the strains of the bacterium as well as carbon isotope distribution of the used D-glucose. Because of the smaller size of an AY-201 cell, their produced cellulose microfibrils were of a minor scale compared with those produced by NQ-5. Therefore, the moving rate of AY-201 strain on NOC was apparently and considerably less than that for NQ-5. In spite of the *A. xylinum* strains, both the motion of a single bacterium and the cellulose production were decelerated by D-glucose-U-$^{13}C_6$. This effect is possibly due to the higher mass of carbon-13 isotopes. In addition, some hints could be demonstrated in order to prove the crystallinity of the deposited cellulose nanofibers on NOC even though their self-aggregation was inhibited by the strong interaction between the biosynthesized cellulose and the NOC surface. The deposited cellulose nanofibers proved to be of a crystalline state similar to the polymorphic state of bacterial cellulose cultivated in the usual HS medium by the assignment in the CP/MAS ^{13}C NMR spectrum. Moreover, a vibrational behavior characteristic for cellulose I was acquired in the Raman spectrum of cellulose fibers.

Acknowledgements

The authors thank Mr E. Togawa (FFPRI Tsukuba) for the preparation of NOC and Dr S. Kimura (FFPRI Tsukuba) for his kind assistance in the cellulose cultivation. Moreover, St H. thanks Ms A. Morohoshi (FFPRI Tsukuba) for her technical assistance through this research and Dr A. Pohlmann (FSU Jena) for the use of the NIR FT Raman spectrometer. This research was made possible by financial support provided by the Friedrich Schiller University of Jena (*Foerderung von Frauen in Forschung und Lehre*, Kapitel 1524/TG 84, 2002) for St.H., by MAFF Nanotechnology Project, Ministry of Agriculture, Forestry and Fisheries and partly by a Grant-in-Aid for Scientific Research (No. 14360101), Japan Society for the Promotion of Science (JSPS) for T.K. The authors are also indebted to Dr U. Sternberg (FZ Karlsruhe) for partly financing D-glucose-U-$^{13}C_6$.

References

Arashida, T., Ishino, T., Kai, A., Hatanaka, K., Akaike, T., Matsuzaki, K., et al. (1993). Biosynthesis of cellulose from culture media containing ^{13}C-labeled glucose as a carbon source. *Journal of Carbohydrate Chemistry*, *12*, 641–649.

Atalla, R. H. (1976). Raman spectral studies of polymorphy in cellulose, part I: Celluloses I and II. *Applied Polymer Symposium*, *28*, 659–669.

Atalla, R. H., & Gast, J. C. (1980). ^{13}C NMR spectra of cellulose polymorphs. *Journal of the American Chemical Society*, *102*(9), 3249–3251.

Atalla, R. H., Ranua, J., & Malcolm, E. W. (1984). Raman spectroscopic studies of the structure of cellulose: A comparison of kraft and sulfite pulps. *TAPPI Journal*, *67*(2), 96–99.

Atalla, R. H., & VanderHart, D. L. (1984). Native cellulose—a composite of two distinct crystalline forms. *Science*, *223*, 283–285.

Blackwell, J., Vasko, P. D., & Koenig, J. L. (1970). Infra-red and Raman spectra of the cellulose from the cell wall of *Valonia ventricosa*. *Journal of Applied Physics*, *41*, 4375–4379.

Brown, R. M., Willison, J. H. M., & Richardson, C. L. (1976). Cellulose biosynthesis in *Acetobacter xylinum*: Visualization of the site of synthesis and direct measurement of the in vivo process. *Proceedings of the National Academy of Sciences of the United States of America (PNAS)*, *73*(12), 4565–4569.

Chanzy, H., Peguy, A., Chaunis, S., & Monzie, P. (1980). Oriented cellulose films and fibers from a mesophase system. *Journal of Polymer Science: Polymer Physics Edition*, *18*(5), 1137–1144.

Earl, W. L., & VanderHart, D. L. (1980). High resolution magic angle sample spinning ^{13}C NMR of solid cellulose I. *Journal of the American Chemical Society*, *102*(9), 3251–3252.

Earl, W. L., & VanderHart, D. L. (1982). Measurement of ^{13}C chemical shifts in solids. *Journal of Magnetic Resonance*, *48*, 35–54.

Emert, G., Gum, E., Lang, J., Liu, T., & Brown, R. (1974). Cellulases. In J. Whitaker (Ed.), *Food related enzymes*. Washington, DC, USA: American Chemical Society.

Erata, T., Shikano, T., Yunoki, S., & Takai, M. (1997). The complete assignment of the ^{13}C CP/MAS NMR spectrum of native cellulose by using ^{13}C labeled glucose. *Cellulose Communications (Japanese)*, *4*, 128–131.

Evans, R. J., Wang, D., Agblevor, F. A., Chum, H. L., & Baldwin, S. D. (1996). Mass spectrometric studies of the thermal decomposition of carbohydrates using ^{13}C-labeled cellulose and glucose. *Carbohydrate Research*, *281*(2), 219–235.

Gagnaire, D., & Taravel, F. R. (1980). Biosynthesis of bacterial cellulose from D-glucose uniformly enriched in ^{13}C (author's translation). *European Journal of Biochemistry*, *103*, 133–143.

Hesse, St., & Jaeger, C. (2005). Determination of the ^{13}C-chemical shift anisotropies of cellulose I and cellulose II. *Cellulose*, *12*, 5–14.

Hesse, St., Togawa, E., & Kondo, T. (in preparation). Structure elucidation of ^{13}C-enriched bacterial cellulose: AFM, NMR, NIR FT Raman, and X-ray studies. *Biomacromolecules*.

Hestrin, S., & Schramm, M. (1954). Synthesis of cellulose by *Acetobacter xylinum*: Preparation of freeze dried cells capable of polymerizing glucose to cellulose. *Biochemical Journal*, *58*, 345–352.

Jaeger, C., Pauli, J., & Schmauder, H.-P. (2003). *Poster: Observation of the glycosidic bond and complete ring assignment of the ^{13}C-signals of bacterial cellulose*. Leipzig: Magnetic Resonance Spectroscopy Division of the German Chemical Society.

Kai, A., Arashida, T., Hatanaka, K., Akaike, T., Matsuzaki, K., Mimura, T., et al. (1994). Analysis of the biosynthetic process of cellulose and curdlan using ^{13}C-labeled glucose. *Carbohydrate Polymers*, *23*, 235–239.

Kai, A., Karasawa, H., Kikawa, M., Hatanaka, K., Matsuzaki, K., Mimura, T., et al. (1998). Biosynthesis of ^{13}C-labeled branched polysaccharides by pestalotiopsis from ^{13}C labeled glucoses and the mechanism of formation. *Carbohydrate Polymers*, *35*, 271–278.

Klemm, D., Schumann, D., Udhardt, U., & Marsch, S. (2001). Bacterial synthesized cellulose—Artificial blood vessels for microsurgery. *Progress in Polymer Science*, *26*, 1561–1603.

Kono, H., Erata, T., & Takai, M. (2003). Determination of the through-bond carbon–carbon and carbon–proton connectivities of the native celluloses in the solid state. *Macromolecules*, *36*, 5131–5138.

Kondo, T., Nojiri, M., Hishikawa, Y., Togawa, E., Romanovicz, D., & Brown, R. M. (2002). Biodirected epitaxial nanodeposition of polymers on oriented macromolecular templates. *Proceedings of the National Academy of Sciences of the United States of America (PNAS)*, *99*(22), 14008–14013.

Kondo, T., Togawa, E., & Brown, R. M. (2001). Nematic ordered cellulose: A concept of glucan chain association. *Biomacromolecules*, *2*(4), 1324–1330.

Kono, H., Yunoki, S., Shikano, T., Fujiwara, M., Erata, T., & Takai, M. (2002). CP/MAS ^{13}C NMR study of cellulose and cellulose derivatives 1. Complete assignment of the CP/MAS ^{13}C NMR spectrum of the native cellulose. *Journal of the American Chemical Society*, *124*(25), 7506–7511.

Lesage, A., Bardet, M., & Emsley, L. (1999). Through-bond carbon–carbon connectivities in disordered solids by NMR. *Journal of the American Chemical Society*, *121*, 10987–10993.

Morohoshi, A., & Kimura, S. (2002). FFPRI Tsukuba, Japan, private communications.

Reese, E., Siu, R., & Levinson, H. (1950). The biological degradation of soluble cellulose derivatives and its relationship to the mechanism of cellulose hydrolysis. *Journal of Applied Bacteriology*, *59*, 485–497.

Schenzel, K., & Fischer, S. (2001). NIR FT Raman spectroscopy—A rapid analytical tool for detecting the transformation of cellulose polymorphs. *Cellulose*, *8*, 49–57.

Seifert, M., Hesse, St., Kabrelian, V., & Klemm, D. (2004). Controlling the water content of never dried and re-swollen bacterial cellulose by addition of water-soluble polymers to the culture medium. *Journal of Polymer Science A: Polymer Chemistry*, *42*(3), 463–470.

Togawa, E., & Kondo, T. (1999). Change of morphological properties in drawing water-swollen cellulose films prepared from organic solutions: A view of molecular orientation in the drawing process. *Journal of Polymer Science B: Polymer Physics*, *37*, 451–459.

VanderHart, D. L., & Atalla, R. H. (1984). Studies of microstructure in native cellulose using solid-state ^{13}C NMR. *Macromolecules*, *17*, 1465–1472.

VanderHart, D. L., & Atalla, R. H. (1987). Further carbon-13 NMR evidence for the coexistence of two crystalline forms in native celluloses. In R. H. Atalla, *The structures of celluloses. ACS Symposium Series* (340) (pp. 88–118). Washington, DC, USA: American Chemical Society, 88–118.

Whitaker, D. (1971). In P. D. Boyer,3rd ed. *The enzymes* (Vol. 5) (p. 273). New York: Academic Press, 273.

Wiley, J. H., & Atalla, R. H. (1987). Band assignments in the Raman spectra of celluloses. *Carbohydrate Research*, *160*, 113–129.